

Research Article

Vibration Reduction of Axially-extending Cantilever Beams under Gravity Using Command Shaping

¹Seong-Wook Hong, ¹Seon-Woong Kwon and ²William E. Singhose

¹Department of Mechanical System Engineering, Kumoh National Institute of Technology, Gumi, Gyeongbuk, Korea

²School of Mechanical Engineering, Georgia Institute of Technology, Atlanta, Georgia, USA

Abstract: This study investigated the dynamics and vibration reduction for axially-extending cantilever beams subjected to gravity. Command shaping on the extension velocity was used to reduce the vertical vibration of the extending beams. Because conventional command shapers have limited effectiveness due to the time-varying properties of the system, this study presented an optimization procedure on the damping and frequency for designing the command shaper. Simulations were performed to analyze the vibration problem and to characterize the performance of the optimized command shaper. Experiments were also performed to validate the proposed, optimal command shaper.

Keywords: Command shaping, extending beams, optimization, residual vibration, vertical vibration

INTRODUCTION

Mechanisms that have extending/retracting cantilever beams, such as telescopic arms, are very useful in manufacturing processes (Zhang and Yang, 2016; Yuan *et al.*, 2014). Such mechanisms are often employed for material-handling processes that perform within limited spaces. Figure 1 shows a telescopic handler mechanism that utilizes extending/retracting beams. As illustrated in Fig. 2, this handler extends its multi-stage beams to pick and place glass wafers in several processing chambers. This mechanism, however, tends to vibrate during the extending and retracting procedure because of its inherent time-varying properties. The vibration during extension of this mechanism needs special attention because it may break the glass wafer.

The dynamics in association with axially-extending/retracting or axially-moving beams have been introduced by several researchers, e.g., Mote (1972) and Tabarrok *et al.* (1974) and then, attracted attention from many researchers through various engineering problems during several decades (Wickert and Mote, 1988; Buffinton, 1992; Al-Bedoor and Khulief, 1996; Theodore *et al.*, 1996; Lee and Park, 2002; Bannerjee and Gunawardana, 2007; Ghayesh *et al.*, 2010; Chang *et al.*, 2010; Yuan *et al.*, 2014). Much research has focused on the dynamics of axially-moving beams with fixed or clamped boundary conditions, which can be applied to band saws, serpentine belts and so on. There have also

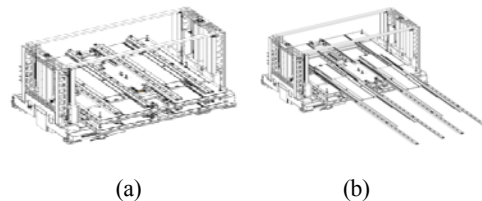


Fig. 1: Robotic telescopic mechanism for glass wafer handling; (a): Before extending; (b): After extending

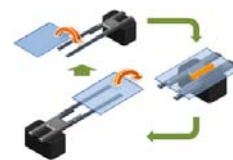


Fig. 2: Illustration of glass handling procedure with the robotic telescopic mechanism

been numerous results concerned with axially-extending/retracting beams, which can be applied to robotic manipulators with prismatic joints, spacecraft antennas and so on.

The defining characteristic of an axially-extending beam is that its length varies. Therefore, most discrete modeling methods that make use of time-invariant elements are not straightforward to apply. To overcome this limitation, the variable domain finite element method was developed for the analysis of axially-moving beams

Corresponding Author: Seong-Wook Hong, Department of Mechanical System Engineering, Kumoh National Institute of Technology, 61 Daehak-Ro, Gumi, Gyeongbuk 730-701, Korea

This work is licensed under a Creative Commons Attribution 4.0 International License (URL: <http://creativecommons.org/licenses/by/4.0/>).

(Stylianou and Tabarrok, 1994; Chang *et al.*, 2010). While many research papers have been published on the dynamic modeling and analysis of axially-moving beams, few papers have been published with regard to suppression of residual vibration in axially-moving beams. It is well known that the gravity makes the system non-homogeneous and plays an essential role as a vertical vibration source for the extending beams (Imanishi and Sugano, 2003; Lim *et al.*, 2011). Thus, a rigorous countermeasure for the gravity-induced vibration is essential for a system that employs axially-extending beams.

This study presents a command shaping method to suppress vertical vibration caused by time-varying characteristics in horizontally-extending beams. There have been few research results regarding the use of command shaping for vibration suppression of horizontally-extending beams. The basic concept used in command shaping is to generate a command whose first component induces vibration, but the later parts of the command cancel the vibration (Singer and Seering, 1990; Singhose and Seering, 2007; Singhose, 2009). Recently, the authors investigated the possibility of vibration suppression for axially-extending beams subjected to gravity by using such a command shaping method (Lim *et al.*, 2011; Hong and Singhose, 2012). In this case, the command shaper modifies the extension velocity profile to cancel out the gravity-induced vibration. The application of command shaping to this problem differs from typical examples of command-shaping applications because the command changes the dynamic properties of the system, as well as the effective force of gravity at the same time. From a series of simulations and experiments, it was found that the conventional-command shaping method can be used, but may not be highly effective (Lim *et al.*, 2011).

Several command-shaping techniques were attempted to reduce residual vibrations in time-varying flexible systems. For slow-varying systems, the robustness of a command shaper can overcome the parametric change in the system to reduce the residual vibration quite well. For example, cranes usually hoist up payloads quite slowly, so command shaping works well to suppress the pendulum swing in the presence of the system's time-varying properties (Singhose *et al.*, 2000). However, for fast-varying systems such as robotic manipulators, time-varying command-shaping techniques have been employed. The time-varying command shaping has proved useful but requires somewhat complicated operation for implementation (Lee and Park, 2002; Rhim and Book, 2004; Park and Chang, 2004). Hong and Singhose (2012) proposed another approach to modify the conventional command shaper to better suppress the residual vibration of a time-varying system.

This study presents a design method for command shapers to cope with the time-varying nature of axially extending beams. The frequency and damping ratio for

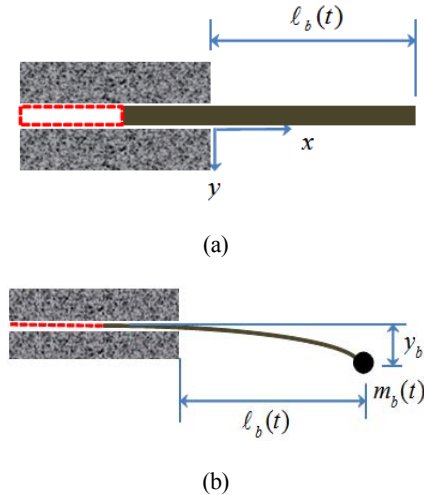


Fig. 3: Schematic diagram of axially-extending beam (Lim *et al.*, 2011); (a): Axially_extending beam; (b): Approximate modal model

the command shaper are selected as design variables to be determined, considering the time-varying nature of the system (Hong and Singhose, 2012). Then, the optimum values were assessed and tested over various extending velocities. To investigate the characteristics of the proposed method, simulations are performed with a single degree-of-freedom time-varying model. Experiments are performed to find and validate the optimal command shaper by using the proposed approach. The experimental results show that the proposed command shaper design is very useful for suppressing the residual vibration of axially-extending beams.

MODELING OF AXIALLY-EXTENDING BEAM

Assumptions and modeling: Because most extending beams behave like a cantilever, one Degree-of-Freedom (DOF) approximations using their fundamental, instantaneous natural frequency reflect their essential characteristics very well. Thus, from a practical point of view, such approximate models are useful for investigating vibration-suppression methods and control algorithms (Imanishi and Sugano, 2003). Figure 3a shows a schematic model of a system investigated in this study. A beam is horizontally-extending with a clamped boundary condition at the left end. The associated modal model simplified with one DOF is shown in Fig. 3b. All the DOFs other than the axial and vertical axes are assumed to be restrained. As indicated in Fig. 3b, the beam stiffness is approximated by the lumped static stiffness at the right end of beam. The distributed mass is also approximated by a modal mass concentrated at the right end of beam. The modal mass value is derived from the equation of instantaneous natural frequency. The mass and stiffness can be obtained as follows (Imanishi and Sugano, 2003; Lim *et al.*, 2011):

Table 1: Simulation parameters

Parameter	Symbol	Value
Material	-	Aluminum
Initial Length	L_0	0.26(m)
Initial Deflection	δ_0	0(m)
Extension velocity	v	0.5(m/s)
Extending Time	Acc/Dec	0.05(s)
	Uniform speed	1(s)
Material Density	ρ	2770(kg/m ³)
Young's Modulus	E	69(GPa)
Cross Section Area	A	0.04×0.002(m ²)
Area moment of inertia	I	0.04×0.002 ³ /12(m ⁴)

$$m_b = \frac{3\rho A \ell_b(t)}{\beta^4}, k_b = \frac{3EI}{\ell_b(t)^3} \quad (1)$$

where, $\ell_b(t)$ is the length of the extended beam, EI is the rigidity of beam and ρ, A are the density and the cross-sectional area of the beam, respectively. β is a non-dimensional number associated with the fundamental natural frequency, in this case, 1.8751.

By applying the Lagrange method to the system with the instantaneous mass and stiffness terms represented in Eq. (1), along with a conservative force term due to gravity, the governing equation can be obtained as (Imanishi and Sugano, 2003; Lim *et al.*, 2011):

$$m_b(t)\ddot{y}_b + \left\{ m_b(t) \frac{\dot{\ell}_b(t)}{\ell_b(t)} + c_b \right\} \dot{y}_b + k_b(t)y_b = \gamma m_b(t)g \quad (2)$$

where g is the gravitational acceleration, c_b is the equivalent damping coefficient other than the self-damping term. γ is a correction factor to compensate for the gravity force, β^4 in this case.

Equation (2) can be rewritten, by dividing by the mass term, as:

$$\ddot{y}_b + 2\zeta(t)\omega_n(t)\dot{y}_b + \omega_n^2(t)y_b = \gamma g \quad (3)$$

where,

$$\omega_n(t) = \sqrt{\frac{k_b(t)}{m_b(t)}} = \frac{\beta^2}{\ell_b^2(t)} \sqrt{\frac{EI}{\rho A}}, \zeta(t) = \frac{1}{2\omega_n(t)} \left\{ \frac{\dot{\ell}_b(t)}{\ell_b(t)} + \frac{c_b}{m_b(t)} \right\} = \frac{\ell_b^2(t)}{2\beta^2} \sqrt{\frac{\rho A}{EI}} \left\{ \frac{\dot{\ell}_b(t)}{\ell_b(t)} + \frac{c_b}{m_b(t)} \right\}$$

From Eq. (3), it is obvious that the system excites itself.

Simulation and problem definition: Figure 4 shows the simulated vertical vibrations during several extending processes that are all performed in 1.1 s. The simulation parameters are listed in Table 1 and the external damping c_b is assumed to give a damping ratio of 0.01. To generate a realistic velocity profile, we use a trapezoidal velocity profile that includes acceleration and deceleration periods of 0.05s. In the Fig. 4, the beam undergoes a significant change in the vibration frequency as it extends. However, when it stops, it vibrates at a constant frequency which is the end-point natural frequency. At the beginning of the extending procedure, the vibration has a very high frequency and small amplitude, but becomes significant at the end of the extension. Increases in extension velocity result in higher amplitude vibration with lower frequency because the command duration time is identical for all the cases. Therefore, the extension velocity is proportional to the extended length of the beam.

One reason for the insignificant vibration in the initial stage is the existence of self-damping induced by time variation of modal mass. However, this damping term vanishes quickly after starting extending procedure and may even destabilize the system during a retracting procedure unless sufficient external damping is provided. When the extending procedure stops, the system becomes time-invariant and the internal self-damping disappears.

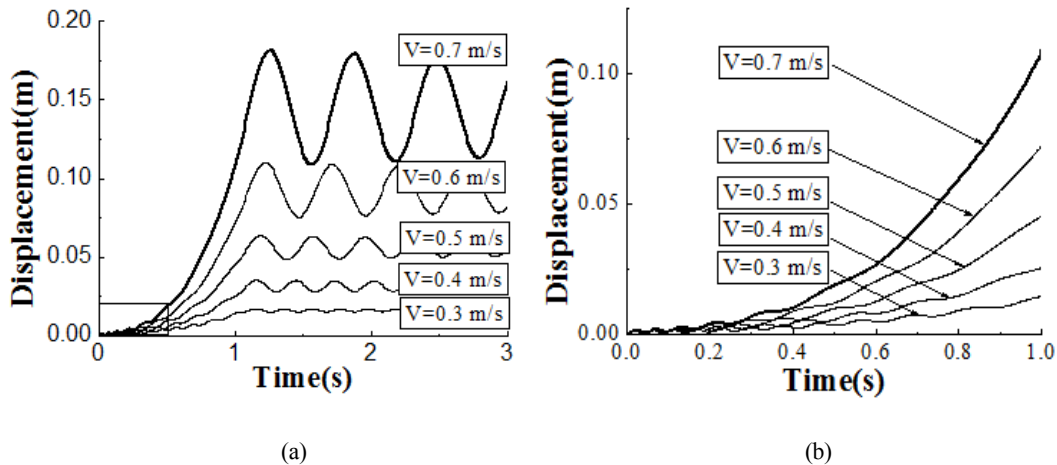


Fig. 4: Beam tip vibrations for various extension velocities: (a): Wide; (b): Zoomed

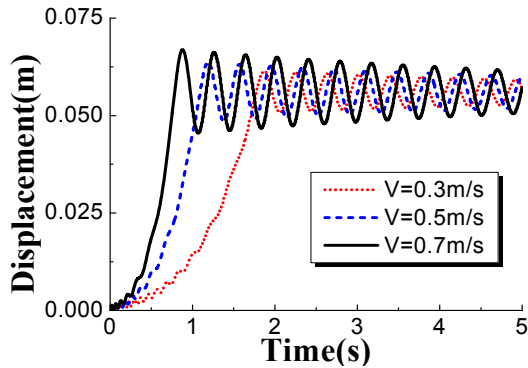


Fig. 5: Beam tip vibrations for various extension velocities subjected to the same final extension length

Another reason for the low vibration in the initial stage is that the natural frequency is very high at small extension lengths.

While the extension velocity explicitly affects the damping term as shown in Eq. (2) and (3), it implicitly changes the other parameters by affecting the extended length of the beam. Thus the effects of extension velocity on the residual vibration are equivalent to those of the extended length of the beam. Figure 5 shows the simulated vertical vibrations of the beam when the extension time period and extension velocity are changed to make the extended length identical. Increasing velocity affects the damping during the extension processes, as well as the amplitude of residual vibration. However, it does not affect the residual vibration frequency and damping characteristics.

Notice here that the extension velocity affects only the mass, damping and stiffness parameters, not the force term on the right side of Eq. (3). Thus, the problem in this case can be defined as how to modify the extension velocity profile or equivalently the extended beam length profile, to remove this vibration.

RESIDUAL VIBRATION REDUCTION BY COMMAND SHAPING

Command shaping is a method to limit the vibration of flexible positioning systems by modifying the input command (Singhose and Seering, 2007). Here, command shaping is applied to the extension velocity of the beam.

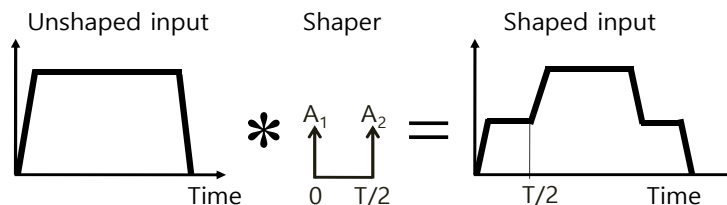


Fig. 6: Command shaping process for extension velocity (Singhose and Seering, 2007)

Even though the gravitational force affecting the beam is proportional to the extended length of the beam, the gravity force itself does not excite the beam, as can be seen in Eq. (3). The parametric changes in the stiffness and damping terms, which are caused by the extending length of the beam, are the source of vibration in this case.

To test the performance of conventional command shapers, the Zero Vibration (ZV) and Zero Vibration and Derivative (ZVD) shapers (Singhose and Seering, 2007), are applied to the system. The command shaper design frequency and damping ratio are set to the end-point natural frequency and 0.01, respectively (Lim *et al.*, 2011). Figure 6 illustrates the ZV-shaping process for a trapezoidal velocity command. $T/2$ is the time interval between impulses, which is half of the fundamental period of vibration.

Figure 7 compares the responses with and without the conventional command shapers. The extension velocity and the end-point natural frequency are set to 0.5m/s and 2.617Hz, respectively. Both the conventional ZV and ZVD command shapers remain a considerable amount of residual vibration: 20.9% for the ZV shaper and 13.4% for the ZVD shaper when compared with that of the unshaped case. However, these results demonstrate that command shaping can reduce the residual vibration for the axially-extending beam under gravity. The conventional command shapers are ineffective because that they do not address the time-varying nature of the system. The next section will deal with how to improve the command-shaping method for the system under consideration.

IMPROVEMENT OF COMMAND SHAPING METHOD

Design variables and performance index: The conventional command shapers require the natural frequency and damping ratio for the mode to be suppressed. However, the natural frequencies and damping ratios are not explicitly defined for time-varying systems. Thus, the end-point natural frequency was used in the previous section. Here, we consider the natural frequency and damping ratio for generating the command shaper as design variables. This approach was proved useful for a system with hysteretic nonlinearity (Bae *et al.*, 2014). Then, the optimum values are estimated to suppress the residual vibrations. A performance index to

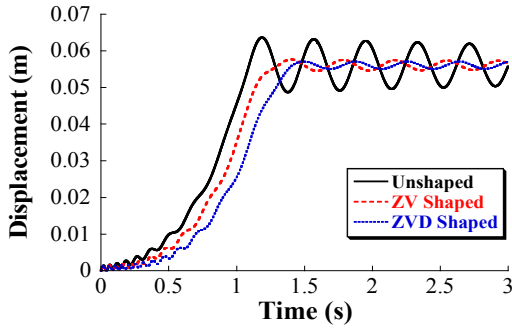


Fig. 7: Time responses with and without conventional command shaping ($v = 0.5\text{m/s}$)

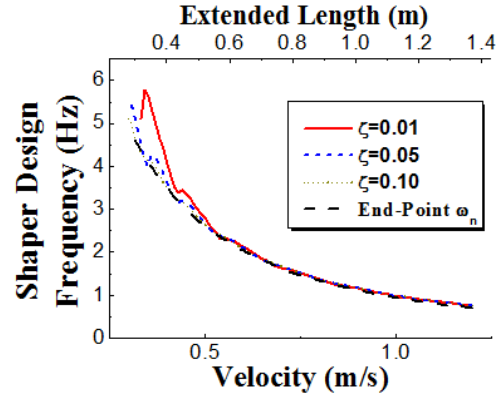


Fig. 10: Optimal frequency for command shaper as a function of extension velocity

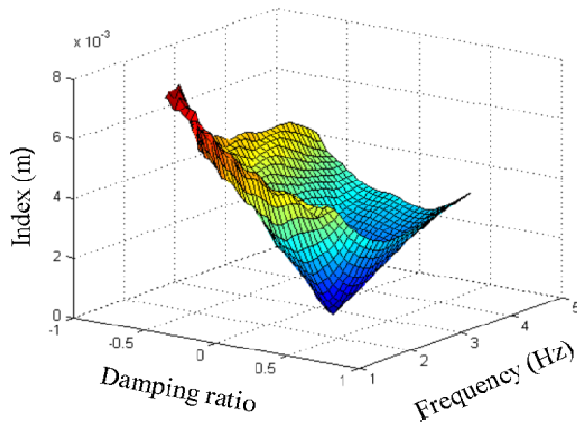


Fig. 8: Performance index as a function of the frequency and damping ratio ($v = 0.5\text{m/s}$)

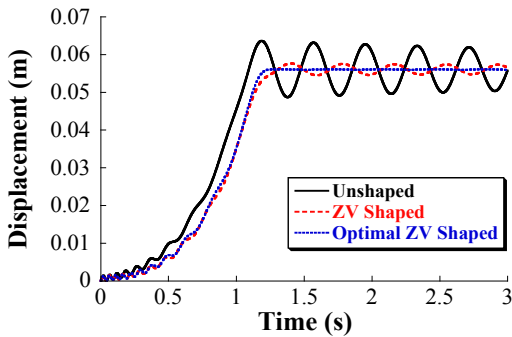


Fig. 9: Responses using the optimal command shaper, the conventional ZV shaper and no command shaping ($v = 0.5\text{m/s}$)

represent the amount of residual vibration is introduced as (Hong and Singhose, 2012):

$$J(f_s, \zeta_s) = \text{abs} \left\{ \begin{array}{l} \max(y_b(t_m : t_f)) \\ - \min(y_b(t_m : t_f)) \end{array} \right\} \quad (4)$$

where, $y_b(t)$ is the time response due to the applied command shaper, t_m and t_f are the starting time and the final time, respectively, to simulate the vibration and to

estimate the performance index. t_m is greater than or equal to the command duration time and t_f should be greater than t_m and presumably the total time is long enough to capture the residual vibration.

Improvement of the command shaper: The simulation parameters used in the previous section are used to obtain and test the improved ZV command shapers. In this case, t_m and t_f are set to the command duration time and 6s, respectively. Figure 8 shows a 3D-plot for the performance index when the frequency f_s and damping ratio ζ_s are varied. It is clearly shown that there exists an optimal combination of the frequency and damping ratio that can minimize the performance index. The optimal frequency and damping ratio are tested by simulation.

Figure 9 shows the time responses when the conventional ZV and ZVD shapers and the improved ZV shapers are applied. Here, the optimal natural frequency and damping ratio for the improved ZV shaper are 2.786Hz and 0.0357, respectively. While the conventional ZV shaper remains residual vibration, the new, improved ZV shaper produces almost perfect performance.

Analysis on optimal ZV shapers: In order to find a general correlation between the system characteristics and the optimal frequency and damping ratio for the command shaper, a parametric study is performed with regard to the extension velocity.

Figure 10 shows the relationship between the extension velocity and the shaper design frequency with the system damping ratio varied. The end-point natural frequency is also shown with the optimal natural frequency for comparison. In the low-velocity region, the optimal shaper frequencies fluctuate, while in the high-velocity region there is little fluctuation and they are close to the end-point natural frequency. The increase of system damping makes the curve smoother. Because this simulation sets the extension time as a constant of 1, higher extension velocities produce longer extension lengths, leading to lower natural frequency.

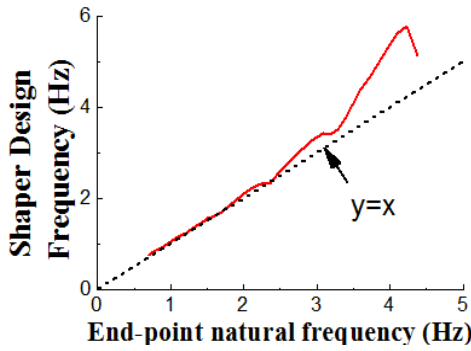


Fig. 11: Comparison of end-point natural frequency and shaper frequency ($\zeta = 0.01$)

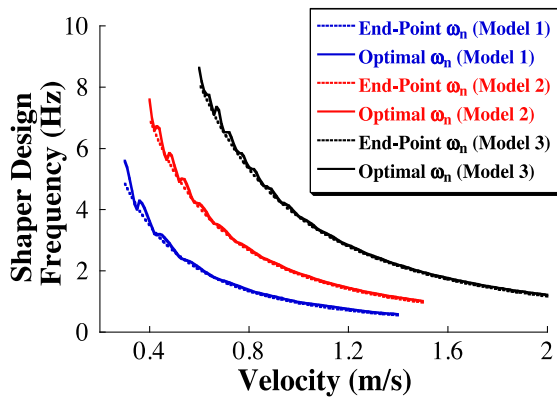


Fig. 12: Optimal shaper frequencies for three models with the beam depth varied (model 1: depth = 2mm, model 2: depth = 4mm, model 3: depth = 8mm)

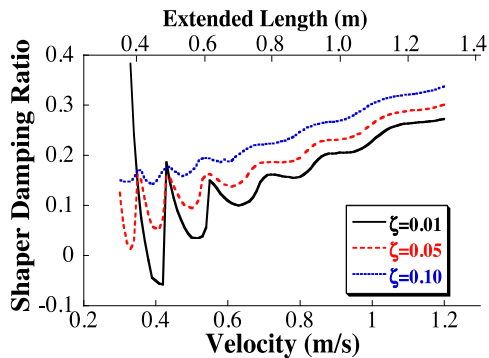


Fig. 13: Optimal damping ratio for command shaper as a function of the extension velocity

Figure 11 shows the relationship between the end-point natural frequency and the optimal shaper frequency for the system with a damping ratio of 0.01. For the low-frequency region, the two frequencies are almost equal. However, in the high-frequency region, the shaper frequency deviates from the linear trend and becomes greater than the end-point natural frequency.

Figure 12 compares the optimal shaper frequencies along with the end-point natural frequencies for three

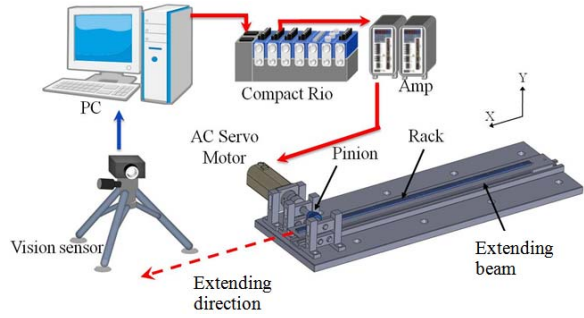


Fig. 14: Schematic diagram of experimental setup (Lim *et al.*, 2011)

models, which have different beam depth. The system damping ratio is assumed to be constant at 0.05. Increases in stiffness do not alter the trend of the optimal shaper frequency with the velocity varied. For the low natural frequency region, the optimal shaper frequency is close to the end-point natural frequency, while the optimal shaper frequency fluctuates in the high natural frequency region.

The optimal shaper damping ratio has similar characteristics as the frequency. Figure 13 shows the relationships between the extension velocity and the optimal shaper damping ratio. It should be noted that the optimal damping ratio can be negative. This simply means that the amplitude of the second impulse in the command shaper is bigger than that of the first impulse. In the case when the system damping ratio is 0.01, the shaper damping ratio is very sensitive to the extension velocity in the low-velocity range. In summary, the optimal shaper frequency and damping ratio are not sensitive to parametric change in the low natural frequency region, but they should be searched very carefully in the high natural frequency region.

EXPERIMENTAL RESULTS AND DISCUSSION

Experimental setup: Experiments were performed to validate the proposed command-shaping method. Figure 14 is a schematic diagram of the experimental system that was used by Lim *et al.* (2011) and Hong and Singhose (2012). A beam is axially driven by a servomotor along with a rack and pinion mechanism. The servomotor is controlled by a motion controller and a LabVIEW program that generates trapezoidal velocity profiles. In this experiment, a tip mass of 100g is attached at the beam tip to make the system more flexible and less affected by external damping. A circular target is attached to the end of the beam. A CCD camera, running at 60 frames per second, is used to track the target via image processing. Figure 15 shows the actual experimental setup. The extending beam is made of an aluminum bar whose width and height are 4cm and 2mm, respectively.

The trapezoidal velocity profile is applied: the extension velocity is 0.4m/s and the acceleration and deceleration time is 50ms and the initial beam length is

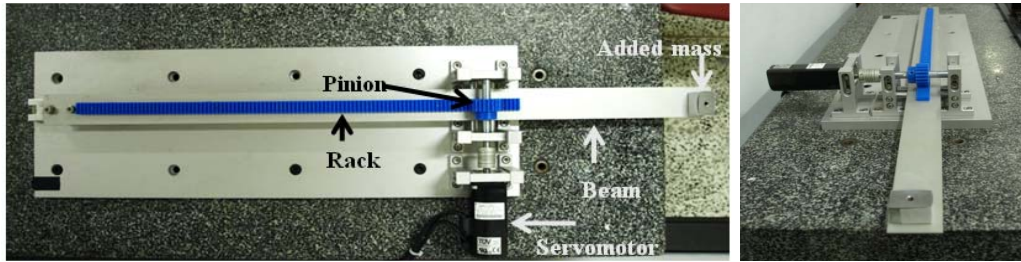


Fig. 15: Experimental setup for axially-extending beam

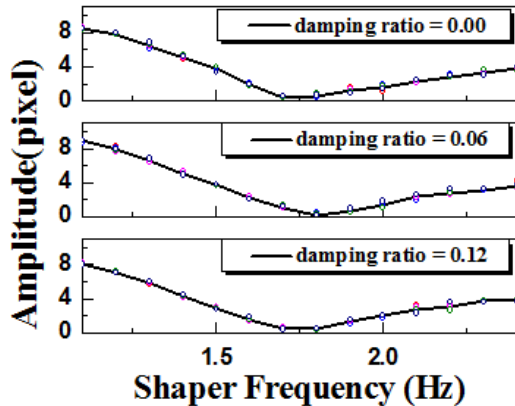


Fig. 16: Experimental results when the shaper natural frequency and damping ratio vary

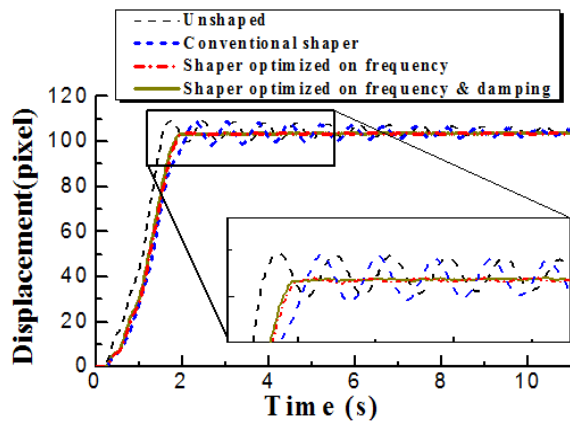


Fig. 17: Experimental responses with three kinds of command shaper and without command shaper

0.27m. The velocity profile was sustained for 1.05 s. The end-point natural frequency was measured as 1.4Hz.

RESULT AND DISCUSSION

Experiments were conducted to find optimal frequency and damping ratio for command shaper under experimental conditions. Figure 16 shows the experimental over-shoot values of vibration at the beam tip as a function of shaper frequency and damping ratio. Experiments were repeated six times to ensure the repeatability of the experimental results. The solid lines are mean values of the experiments and the circles are

individual values. It is clearly shown that the change of shaper frequency and damping ratio affects the responses. In this case, however, the damping ratio is less significant compared to the shaper frequency. The shaper frequency at which over-shoot value becomes minimal is around 1.8Hz, which is different from the end-point natural frequency of 1.4Hz. Based on this figure, the shaper frequency and damping ratio are selected as 1.8Hz and 0.06, respectively. Figure 17 shows time responses with the shapers designed differently. This figure demonstrates that the conventional ZV shaper is not effective, but that the optimal shaper with the frequency of 1.8Hz and the damping ratio of 0.06 performs well at eliminating the residual vibration.

Another optimal shaper with a design frequency of 1.7Hz and no damping ratio is compared with others in Fig. 17. In this case, this command shaper also performs very well. As illustrated here and in the numerical simulation, the optimal shaper frequency is likely to be a little higher than the end-point natural frequency, implying that the equivalent time-varying nature of the system natural frequency is constrained by the end-point natural frequency, which is the lowest.

These figures confirm that the proposed command-shaping method performs well for the vibration suppression of axially-extending beams subjected to gravity. As already discussed, the conventional command shapers do not work well for long and fast extension motions. If more robust shapers such as the EI shaper (Singhose and Seering, 2007) were employed, the result may be better. However, robust shapers necessitate longer rise time. The command shaper proposed here is based on the simple ZV shaper and does not increase the rise time significantly. On the other hand, the proposed design method for command shaper may be further used for other time-varying systems.

CONCLUSION

This study presented a method to design an optimal command shaper for suppressing residual vibration in horizontally-extending beams subjected to gravity. Unlike the conventional command shaper, the natural frequency and damping ratio used to generate for the command shaper were treated as design variables to cope with the time-varying nature of the system. The design variables were optimized to minimize the residual vibration. An extensive parametric study regarding the optimal

command shaper was also performed. The proposed optimal command shapers were proved to work very well for reducing the residual vibration of horizontally-extending beams in both simulation and experiments.

ACKNOWLEDGMENT

This research has been financially supported by the Research Fund of Kumoh National Institute of Technology.

Conflicts of interest: No conflict of interest on this study.

REFERENCES

- Al-Bedoor, B.O. and Y.A. Khulief, 1996. Vibrational motion of an elastic beam with prismatic and revolute joints. *J. Sound Vib.*, 190(2): 195-206.
- Bae, G.H., S.W. Hong and D.W. Lee, 2014. A study on precision stage with displacement magnification mechanism using flexure-based levers. *Res. J. Appl. Sci. Eng. Technol.*, 7(11): 2225-2231.
- Bannerjee, J.R. and W.D. Gunawardana, 2007. Dynamic stiffness matrix development and free vibration analysis of a moving beam. *J. Sound Vib.*, 303(1-2): 135-143.
- Buffinton, K.W., 1992. Dynamics of elastic manipulators with prismatic joints. *J. Dyn. Syst-T. ASME*, 114(1): 41-49.
- Chang, J.R., W.J. Lin, C.J. Huang and S.T. Choi, 2010. Vibration and stability of an axially moving Rayleigh beam. *Appl. Math. Model.*, 34(6): 1482-1497.
- Ghayesh, M.H., M. Yourkhani, S. Balar and T. Reid, 2010. Vibrations and stability of axially traveling laminated beams. *Appl. Math. Comput.*, 217(2): 545-556.
- Hong, S.W. and W. Singhose, 2012. Command shaper design for transverse vibration suppression of axially-extending cantilever beams under gravity. *Proceeding of the 9th International Conference on Sound and Vibration*. Vilnius, Lithuania.
- Imanishi, E. and N. Sugano, 2003. Vibration control of cantilever beams moving along the axial direction. *Int. J. Series C*, 46(2): 527-532.
- Lee, K.S. and Y.S. Park, 2002. Residual vibration reduction for a flexible structure using a modified input shaping technique. *Robotica*, 20(5): 553-561.
- Lim, J.G., W.S. Yoon, H.R. Beom and S.W. Hong, 2011. A study on suppression of lateral vibration for axially deploying beams under gravity. *J. Korean Soc. Precis. Eng.*, 28(8): 959-965.
- Mote, C.D. Jr., 1972. Dynamic stability of axially moving materials. *Shock Vib. Digest*, 4(4): 2-11.
- Park, J.Y. and P.H. Chang, 2004. Vibration control of a telescopic handler using time delay control and commandless input shaping technique. *Control Eng. Pract.*, 12(6): 769-780.
- Rhim, S. and W.J. Book, 2004. Adaptive time-delay command shaping filter for flexible manipulator control. *IEEE-ASME T. Mech.*, 9(4): 619-626.
- Singer, N.C. and W.P. Seering, 1990. Preshaping command inputs to reduce system vibration. *J. Dyn. Syst. Meas. Control*, 112(1): 76-82.
- Singhose, W., 2009. Command shaping for flexible systems: A review for the first 50 years. *Int. J. Precis. Eng. Manuf.*, 10(4): 153-168.
- Singhose, W. and W. Seering, 2007. *Command Generation for Dynamic Systems*. William Singhose, Atlanta, GA.
- Singhose, W., L. Porter, M. Kenison and E. Kriikku, 2000. Effects of hoisting on the input shaping control of gantry cranes. *Control Eng. Pract.*, 8(10): 1159-1165.
- Stylianou, M.C. and B. Tabarrok, 1994. Finite element analysis of an axially moving beam, Part 1: Time integration. *J. Sound Vib.*, 178(4): 433-453.
- Tabarrok, B., C.M. Leech and Y.I. Kim, 1974. On the dynamics of an axially moving beam. *J. Franklin Inst.*, 297(3): 201-220.
- Theodore, R.J., J.H. Arakeri and A. Ghosal, 1996. The modelling of axially translating flexible beams. *J. Sound Vib.*, 191(3): 363-376.
- Wickert, J.A. and C.D. Jr. Mote, 1988. Current research on the vibration and stability of axially moving materials. *Shock Vib. Digest*, 20(5): 3-13.
- Yuan, J., W. Wan, K. Chen, Q. Fang and W. Zhang, 2014. Design and prototyping a cable-driven multi-stage telescopic arm for mobile surveillance robots. *Proceeding of the IEEE International Conference on Robotics and Biomimetics*. Bali, Indonesia, pp: 1845-1850.
- Zhang, L. and Y. Yang, 2016. A Novel Linear Telescopic Mechanism: Configuration and Position Precision Analysis. In: Ding, X. *et al.* (Eds.), *Advances in Reconfigurable Mechanisms and Robots II*. Springer International Publishing, Switzerland, pp: 1107-1117.